# Journal of Plankton Research

academic.oup.com/plankt



J. Plankton Res. (2021) 43(1): 85-102. First published online December 22, 2020 doi:10.1093/plankt/fbaa060

### ORIGINAL ARTICLE

# Annual phytoplankton succession results from niche-environment interaction

MARIARITA CARACCIOLO 1.\*, GRÉGORY BEAUGRAND<sup>2,3,4,\*</sup>, PIERRE HÉLAOUËT<sup>4</sup>, FRANCOIS GEVAERT<sup>3</sup>,
MARTIN EDWARDS<sup>4,5</sup>, FABRICE LIZON<sup>3</sup>, LOÏCK KLÉPARSKI<sup>3,4</sup> AND ERIC GOBERVILLE<sup>6</sup>
'sorbonne université, cnrs, station biologique de roscoff, umr 7144, ecomap, place georges teissier, 29680 roscoff, france, 'centre national de la recherche scientifique (cnrs), université de lille, université littoral côte d'opale, umr 8187, log, laboratoire d'océanologie et de géosciences, f 62930 wimereux, france, 'université de lille, cnrs, univ. littoral côte d'opale, umr 8187, log, laboratoire d'océanologie et de géosciences, f 62930 wimereux, france, 'marine biological association, citadel hill, plymouth pl1 2pb, uk, 'school of biological and marine sciences, university of plymouth, drake circus, plymouth, pl4 8aa, united kingdom and 'unité biologie des organismes et écosystèmes aquatiques (borea), muséum national d'histoire naturelle, sorbonne université, université de caen normandie, université des antilles, cnrs, ird, cp53, 61, rue buffon 75005 paris, france

\*corresponding authors: mariarita.caracciolo@sb-roscoff.fr (mariarita caracciolo) and gregory.beaugrand@univ-lille.fr (gregory beaugrand)

Received February 29, 2020; editorial decision November 12, 2020; accepted November 16, 2020

Corresponding editor: Lisa Campbell

Annual plankton succession has been investigated for many decades with hypotheses ranging from abiotic to biotic mechanisms being proposed to explain these recurrent patterns. Here, using data collected by the Continuous Plankton Recorder (CPR) survey and models originating from the MacroEcological Theory on the Arrangement of Life, we investigate Annual Phytoplankton Succession (APS) in the North Sea at a species level. Our results show that this phenomenon can be predicted well by models combining photosynthetically active radiation, temperature and macronutrients. Our findings suggest that APS originates from the interaction between species' ecological niches and the annual environmental fluctuations at a community level. We discuss our results in the context of traditional hypotheses formulated to explain this recurrent pattern in the marine field.

KEYWORDS: annual plankton succession; phenology; ecological niche; environment; plankton; continuous plankton recorder (CPR); METAL theory

#### INTRODUCTION

Annual Phytoplankton Succession (APS) is defined as the recurrent pattern of species abundance, observed during the annual cycle (Cushing, 1959; Winder and Cloern, 2010; Sommer et al., 2012; Romagnan et al., 2015). In temperate and polar biomes, phytoplankton abundance varies from periods of proliferation in spring and autumn to periods of decline in summer and winter. In subtropical and tropical waters where seasonal changes in solar radiation and temperature are less prominent, plankton abundance is more stable at an annual scale (Dakos et al., 2009).

APS has been widely described in marine ecosystems, leading to a variety of potential explanations often based on mechanisms such as bottom-up (i.e. nutrients availability; Metaxas and Scheibling, 1996) to top-down control (i.e. grazing by organisms such as zooplankton and fish; Sverdrup, 1953; Margalef, 1978; Sommer et al., 1986, 2012; Huisman et al., 1999; Behrenfeld, 2010; Chiswell, 2011; Smyth et al., 2014; Chiswell et al., 2015; Romagnan et al., 2015; Atkinson et al., 2018). Gilbert et al. (2012), Barton et al. (2014) and Romagnan et al. (2015) have provided evidence for a strong influence of the physical environment on phytoplankton dynamics, suggesting a bottom-up control of annual succession. A substantial impact of species interaction, such as grazing that imposes a top-down control (e.g. mesozooplankton species on protists), has also been suggested in the western part of the English Channel (Fileman et al., 2010; Kenitz et al.,

The seasonal cycles of irradiance, temperature and stratification—and associated changes in the pycnocline, thermocline and halocline—are known to be closely related to the onset of phytoplankton growth (Longhurst, 1998), with nutrients influencing the phytoplankton bloom extent (Sommer et al., 2012). Although APS starts typically by the onset of the spring bloom in most extra-tropical regions, winter is a key period during which the ingredients needed to trigger the start of phytoplankton proliferation are prepared (Sommer et al., 2012). During winter, wind intensifies the mixing of the upper layers and an increase in convection leads to a deep mixing leading to an increase in the concentration of nitrate, phosphate and silicate in the surface layers (Falkowski and Oliver, 2007; Mann and Lazier, 1996) while diluting phytoplankton in the water column (Behrenfeld, 2010).

The main objective of this study is to reconstruct APS using models of increasing complexity—generated from the MacroEcological Theory on the Arrangement of Life (METAL; Beaugrand, 2015a)—that considers a set of environmental parameters known to influence marine

phytoplankton dynamics such as temperature, photosynthetically active radiation (PAR) and macro-nutrients. The METAL framework unifies behavioural, physiological, phenological biogeographic and long-term community shifts and consequently allows one to model how communities form and how they are altered by environmental fluctuations, including climatic variability and global climate change (Beaugrand et al., 2010, 2014, 2018; Beaugrand, Mackas, et al., 2013). The strength of this approach is to consider that basic organization and sensitivity of communities can be predicted from simple founding principles. Even though ecosystems are complex adaptive systems (Levin and Lubchenco, 2008), a significant proportion of the spatial and temporal adjustments of marine communities are deterministic, which opens the way to testable predictions. In this study, our objectives are to test whether APS is related to the interaction between the ecological niche (sensu Hutchinson, 1957) of species and seasonal environmental fluctuations, and to identify the key ecological variables of the niche that control annual phytoplankton dynamics.

Using data from the Continuous Plankton Recorder (CPR) survey (Reid et al., 2003), we characterize APS in an area of the North Sea ranging from 1 E to 4 E and from 54°N to 56°N (Fig. S1). The area of consideration is close to the Flamborough Frontal structure, which separates seasonally thermally stratified water to the north and tidally mixed water to the south (Huthnance, 1991; Pingree et al., 1978). We model APS using METAL, comparing observed and predicted patterns, and we investigate how natural environmental fluctuations drive phytoplankton seasonality from initiation to termination. Finally, we discuss our results in the context of APS. including the spring bloom (Widdicombe et al., 2010; Sommer et al., 2012; Romagnan et al., 2015).

#### **METHOD**

#### Biological data

Biological data are originated from the CPR (www.cprsu rvey.org/data/our-data/) survey, a marine monitoring programme currently operated by the Marine Biological Association (MBA) that has sampled the North Atlantic Ocean and its adjacent seas since 1946 on a routine monthly basis and at  $\sim$ 7–10 m depth (Reid et al., 2003). Extensively used in the literature, this dataset has allowed researchers to (i) investigate APS (e.g. Colebrook, 1979, 1982; Zhai et al., 2013; Barton et al., 2014); (ii) characterize pelagic biodiversity (e.g. Barnard et al., 2004; Beaugrand et al., 2002); (iii) document distributional, phenological and physiological responses of marine species to climate change (e.g. Beaugrand et al., 2009; Helaouët

and Beaugrand, 2009; Thackeray et al., 2016; Beaugrand and Kirby, 2018) and (iv) anticipate the consequences of global warming in the pelagic realm (e.g. Reid et al., 1998; Beaugrand et al., 2015).

Here, we focused our analyses on the phytoplankton community of the North Sea (l-4 E and 54-56 N; Fig. S1) and considered 90 species/taxa commonly monitored by the CPR survey over the period 1958-2016 (Table 1). The area was selected for both a regular sampling effort over the study period and its geographical location far from the coast. For each species/taxa, we calculated a daily climatology of species abundances, based on 60 years of sampling.

#### Environmental data

Nutrient data originated from the World Ocean Atlas 2013 V2 provided by the NOAA National Centers for Environmental Information, Silver Spring, MD, USA (www.nodc.noaa.gov/OC5/woa13/woa13data.html; Garcia et al., 2014). It is a scientifically quality-controlled database of historical in situ surface and subsurface phosphate ( $\mu$ mol. L<sup>-1</sup>), silicate ( $\mu$ mol. L<sup>-1</sup>) and nitrate (µmol. L<sup>-1</sup>) measures. Monthly means are provided on a 3D grid of 1° latitude by 1° longitude, by 37 depth levels. We calculated the average nutrient concentrations in the area over the first 20-m water depth. From nitrate and phosphate concentration, we calculated the N/P ratio (Redfield, 1958) known to influence the APS (Falkowski et al., 2000).

We used PAR (Einstein.m<sup>-2</sup>.day<sup>-1</sup>), solar radiation spectrum in the wavelength range of 400–700 nm as a proxy of the level of energy that can be assimilated by photosynthetic organisms (Asrar et al., 1989). Data were provided by the Giovanni online data system, developed and maintained by the NASA GES DISC (gdata1.sci. gsfc.nasa.gov/daac-bin/G3/gui.cgi?instance id=ocea n month). A monthly climatology of PAR, at a spatial resolution of 9 km, was calculated by compiling Seaviewing Wide Field-of-View Sensor (SeaWiFS) data from 2009 to 2012.

We also examined annual changes in the Mixed Layer Depth (MLD in meters; Fig. S2), using data from the Global Ocean Physical Reanalysis product (GLOBAL REANALYSIS PHY 001 030) provided by the Copernicus Marine Environment Monitoring service (https://marine.copernicus.eu/).

We assessed the thermal environment of the 90 phytoplankton species over our region of interest using Sea Surface Temperature (SST) from the Optimum Interpolation (OI), which is based on both in situ and satellite observations (see Reynolds et al., 2002 for a full description of the OI analysis). While nutrients and PAR were

only available at a monthly scale, daily SST allowed us to calculate daily species thermal preferendum: we first calculated daily SSTs on a 1° by 1° grid from January 1982 to December 2017, and then averaged data for the region ranging from 1 E to 4 E and from 34 N to 56 N (Fig. S1). Annual environmental changes are shown in

#### The macroecological theory on the arrangement of life

The METAL is a theory that explains how life is arranged and how changing environmental conditions alter biological arrangements in space and time at different ecological levels (e.g. species, community and ecosystem), allowing predictions to be tested (Beaugrand, 2015a). METAL posits that many ecological (e.g. phenology), biogeographic (e.g. LBGs) and climate-change biology patterns (e.g. phenological and biogeographical shifts) originate from the fundamental niche-environment interaction and unifies a large number of patterns observed in biogeography and ecology at different organizational levels (e.g. spatial range, Rapoport's rule, phenology, latitudinal biodiversity gradients, and formation and alteration of species assemblages) and in climate change biology (e.g. phenological shifts, year-to-year to decadal changes in species abundance, range shift, biodiversity shifts, community alteration and abrupt community shifts; Beaugrand, Rombouts, et al., 2013; Beaugrand et al., 2014, 2018, 2019, 2020; Beaugrand, 2015a, 2015b; Beaugrand and Kirby, 2018).

The theory uses the concept of the ecological niche sensu Hutchinson (1957) as a macroscopic elementary brick to understand how species fluctuate in time and space and how communities form and are altered by environmental fluctuations, including climate change (Fig. 1). All species have an ecological niche, which means that they operate within a range of ecological conditions that are suitable for growth and reproduction. The environment acts by selecting species that have the most suitable niche. It follows that this mechanism determines the place where a species lives (i.e. spatial distribution), time when it is active (i.e. phenology) and how individual density fluctuates from short- to long-time scales. Locally however, the absence of a species may be explained by species interaction and random processes, such as those discussed in the Unified Neutral Theory of Biodiversity and Biogeography (Hubbell, 2001). The ecological niche, measured by the abundance plotted as a function of some key ecological factors throughout the spatial range of a species, integrates all genetic variations that affect biological traits and physiological processes. More information

Table 1: List of phytoplankton species and their correlation with the first three PCs. List of phytoplankton species considered in our study area (see Fig. S1).

Category	Phytoplankton species	PC1 (26.86 %)	PC2 (18.06 %)	PC3 (12.22 %)
Phylum: Ochrophyta	. Tytopiainton oposios	. 0. (20.00 %)	. 02 (10.00 %)	. 55 (12.22 %)
Class: Bacillariophyceae				
1	P. sulcata			X
2	S. costatum	Χ	X	^
3	Thalassiosira spp.		X	
4	D. antarcticus	X		
5	Rhizosolenia styliformis		Χ	
6	Rhizosolenia hebetata semispina		Χ	
7	Chaetoceros(Hyalochaete) spp.		Χ	
8	Chaetoceros(Phaeoceros) spp.		Χ	
9	Odontella sinensis			X
10	Thalassiothrix longissima		X	
11	T. nitzschioides	X		
22	Asteromphalus spp.			
23	Bacteriastrum spp.	Χ		X
24	B. malleus	X		X
25	B. alternans			Χ
26	Odontella aurita	X		
27	Odontella granulata			
28	Odontella regia	X	X	
29	Odontella rhombus			
30	Cerataulina pelagica			
31	C. concinnus		X	
32	Coscinodiscus spp. (Unidentified)	X	X	
33	D. brightwellii	Χ	X	
34	Eucampia zodiacus	.,	X	X
35	Fragilaria spp.	X		
36	G. flaccida			
37	Gyrosigma spp.	V	X	
38	Leptocylindrus danicus	X	V	
39	Navicula spp.		X	
40	Cylindrotheca closterium		X	
41 42	Rhaphoneis amphiceros			
43	Rhizosolenia bergonii Rhizosolenia setigera		X	
44	Stephanopyxis spp.		^	X
48	Nitzschia spp. (Unidentified)			^
49	Odontella mobiliensis			X
64	Proboscia alata	Х		^
65	Leptocylindrus mediterraneus	X		Х
66	Proboscia inermis	^		^
67	Asterionellopsis glacialis		Х	
68	Ephemera planamembranacea		Λ	
69	Pseudo-nitzschia delicatissima complex		Х	
70	Pseudo-nitzschia seriata complex		X	
72	Guinardia delicatula		*	
73	Dactyliosolen fragilissimus		X	
74	G. striata	Χ	= =	
76	Lauderia annulata		Х	
77	Bacillaria paxillifera	X	= =	
78	Corethron hystrix	X		
79	Proboscia curvirostris		Χ	
80	Proboscia indica	X		Χ
81	Rhizosolenia imbricata	Χ		
75	Helicotheca tamesis			

Continued

Table 1 Continued

Category Phylum: Ochrophyta Class: Bacillariophyceae	Phytoplankton species	PC1 (26.86 %)	PC2 (18.06 %)	PC3 (12.22 %)
Class: Dictyochophyceae				
47	Silicoflagellates	X		X
Phylum: Dinoflagellata				
Class: Dinophyceae				
12	C. fusus	X		
13	C. furca	X		
14	Ceratium lineatum	X		
15	Ceratium tripos	X		
16	Ceratium macroceros	X		X
17	Ceratium horridum	X		
18	Ceratium longipes	X		
19	Ceratium arcticum	X		
20	Dinoflagellate cysts (Total)	X		X
21	Polykrikos schwartzii cysts	X		
50	Ceratium arietinum			
51	Ceratium bucephalum			
52	Ceratium buceros			
53	Ceratium carriense			
54	Ceratium hexacanthum	X		
55	Ceratium massiliense	X		
56	Ceratium minutum			X
57	Ceratium teres			
58	Dinophysis spp. Total	X		
59	Oxytoxum spp.			
60	Protoperidinium spp.	X		
61	Pronoctiluca pelagica			
62	Prorocentrum spp. Total	X		
63	Noctiluca scintillans	X		
Philum: Haptophyta				
Class: Prymnesiophyceae				
45	Phaeocystis pouchetii			
46	Coccolithaceae (Total)	X		
Phylum: Cyanobacteria				
Class: Cyanophyceae				
71	Trichodesmium spp.			

The 81 species were grouped in the following classes: 1: Bacillariophyceae, 2: Dinophyceae, 3: Primnesiophyceae, 4: Dictyochophyceae and 5: Cyanophyceae. The first three PCs considered in Fig. 3 and their eigenvalues are reported here. A cross indicates a significant correlation (>|0.5|) between a species and a PC. Some species were not correlated. The percentage of explained variance per PC is indicated into brackets. The seasonal cycles of each phytoplankton species are represented on Fig. 6 (see species numbers, first column of this table, for correspondence).

on METAL can be found in Beaugrand (Beaugrand, 2015a; Beaugrand et al., 2020).

#### Summary of the numerical procedures

In this paper, we specifically test whether APS originates from the interaction between the ecological niche of a species and environmental fluctuations. First (Step 1 hereafter), we examined APS in the North Sea by means

of a Principal Component Analysis (PCA) using data from the CPR survey. APS has been regularly investigated by applying this multivariate technique (Colebrook, 1979, 1984; Beaugrand et al., 2000). A total of 81 species belonging to different taxonomic groups (e.g. diatoms, dinoflagellates) were considered in this analysis. Secondly (Step 2), we created a large pool of (Gaussian) ecological niches using a model from the METAL theory and a growing number of ecological dimensions up to five (i.e.

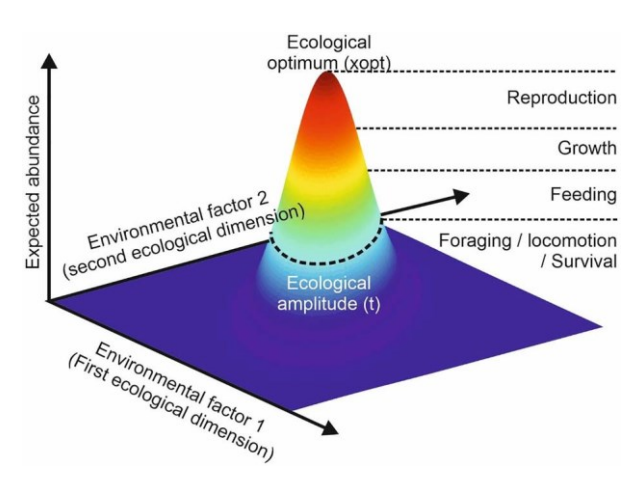


Fig. 1. Representation of a hypothetical 2D ecological niche of a species. The ecological amplitude is an estimation of the breadth of the species' niche and the ecological optimum is the combination of the environmental factors that are optimal for growth and reproduction. Here, the niche is based on a bi-normal distribution with a correlation coefficient fixed to 0.6 between the two environmental factors. At the optimal part of the niche, all biological processes are operational. When ecological conditions become less favorable, this successively impairs reproduction, growth, feeding and survival. Ecological dimensions (i.e. the number of ecological variables) varied between 2 and 5 in this study.  $X_{\text{opt}}$  and t (parameters of Equations 1 and 2) are indicated on the figure.

environmental parameters, Fig. S2). Six environmental parameters were used (e.g. SST, PAR, nitrate, silicate, phosphate and nitrate/phosphate ratio). Thirdly (Step 3), we made 84 simulations building for each a large number of hypothetical ecological niches based on 1-5D niches. All possible niches were therefore built. The maximum abundance of each niche was fixed to 1 and decreasing abundance around the optimum was a function of the environmental amplitude. Estimations of seasonal changes in pseudo-species abundance were calculated at a daily scale by performing a cubic interpolation of the 1-5D niches with the corresponding environmental variables. This calculation step is fully described in Beaugrand and Kirby (2018) (their Fig. 4). We detailed this stage of the procedure in Figs 3 and 4 using simple examples. Fourthly (Step 4), we compared modelled and observed annual patterns in phytoplankton abundance at the species level by means of correlation analyses and the computation of Minimum Assessment Errors (MAEs). To consider a possible bias induced by temporal autocorrelation, we tested both correlations and MAEs with null models.

#### Step 1: Examination of APS from the CPR survey

We first removed species with average annual abundances < 0.5 in the study area, leading to the selection of 81 phytoplankton species (Table 1) for which we estimated average daily abundances for the period 1946–2015. To minimize short-term fluctuations and to reduce the noise inherent to these data, we applied twice a sixth-order symmetrical moving average on each daily time series (Legendre and Legendre, 1998).

A standardized PCA (Jolliffe, 1986) was applied on the correlation matrix [81 phytoplankton species x 365 days] and the significant principal components (PCs) were examined to identify changes in annual plankton succession. Species were then sorted according to their phenology by using normalized eigenvectors, i.e. linear correlation values with the corresponding PCs higher than |0.5| (Table 1). Only significant axes (PCs) that best explained APS were considered (Fig. 3). We tested the significance of the first three axes by using a brokenstick distribution based on 100 000 simulations (Frontier, 1976; Beaugrand et al., 2019). Phytoplankton species were then clustered into five groups: Bacillariophyceae, Dinophyceae, Primnesiophyceae, Dictyochophyceae and Cyanophyceae. We reported here the three PCs for which we found correlations between dominant phytoplankton species and PCs (Table 1).

#### Step 2: Generation of pseudo-species using models from the METAL theory

We modelled the patterns of APS using METAL. First, and using each environmental parameter (i.e. nutrients, PAR and SST), we generated a pool of 1D niches (i.e. niches with only one ecological dimension) based on a Gaussian model (Gauch et al., 1974; Ter Braak, 1996) to calculate species abundance, (Fig. S2)

$$A = c e^{-\frac{\mathbf{f}_{(x-x_{opt})^2}}{2t^2}}$$
 (1)

where A is the abundance of a species as a function of the value of a given environmental parameter x; c the maximum abundance of a pseudo-species with ¢ being fixed to 1 (Beaugrand, 2015b); x<sub>opt</sub> the environmental optimum (e.g. the condition for which a given species reaches the highest level of abundance; Fig. S2) and t the ecological amplitude (i.e. the environmental range where a species can occur; Fig. S2) of a pseudo-species (Table S2). One dimension of the niche (or one ecological dimension; Fig. S2) is represented by the whole range of values of an ecological variable.

Multi-dimensional niches (i.e. niches with more than one ecological dimension) were modelled as follows:

$$A = ce^{-\frac{1}{2}r(\frac{x_1 - x_{opt1}}{t_1})_2 + \dots + (\frac{x_n - x_{optn}}{t_n})_2}, \qquad (2)$$

with  $2 \le n \le 5$  ecological dimensions,  $x_1$  to  $x_n$ , the values of the environmental parameters,  $X_{opt1}$  to  $X_{optn}$ , the optimum values of  $x_1$  to  $x_n$  and  $t_1$  to  $t_n$ , the ecological amplitudes of  $x_1$  to  $x_n$ . c is the maximum abundance of a pseudo-species with ¢ being fixed to 1 (Beaugrand, 2015b). We chose a multiplicative model to ensure that one dimension can exclusively control the abundance of a pseudo-species. For example, if the interaction between the silicate niche and the environment leads to a nil or (low) abundance, the abundance will remain nil (or low) whatever the values of the other ecological dimensions. Simulated ecological niches had five ecological dimensions at maximum. We used six ecological variables to build the different niches: (i) SST, (ii) PAR, (iii) nitrate, (iv) phosphate, (v) silicate and (vi) the N/P ratio. When the N/P ratio was considered, neither nitrate nor phosphate concentrations were included in the niches to avoid possible bias related to multi-collinearity. To examine the sensitivity of our analyses to low PAR conditions, three minimum values were considered (Table S2): 1 (termed 'PARa'), 10 ('PARb') and 20 ('PARc') E.m<sup>-2</sup>.day<sup>-1</sup>.

#### Step 3: Model simulations

We then performed simulations using all possible environmental combinations, from one to five ecological dimensions, leading to a total of 84 runs: 16 simulations based on 1D niches, 23 simulations based on 2D niches, 29 simulations based on 3D niches, 13 simulations based on 4D niches and 3 simulations based on 5D niches (Table S1). The characteristics (optimum and ecological amplitude) of all niches are presented in Table S2. For example, we defined 7 optimum values for temperature (i.e. values corresponding to the highest abundance for a given pseudo-species) from 0 to 36° C—by increment of 6° C—and 4 ecological amplitudes from 1 to 10° C—by increment of  $3^{\circ}$ C—leading to the creation of  $28 (7 \times 4)^{\circ}$ virtual (or pseudo-) niches.

The core principle of METAL is to generate a large number of pseudo-niches (i.e. simulated niches, we say niche hereafter) and pseudo-species (i.e. virtual species; Beaugrand et al., 2020) to examine whether the nicheenvironment interaction (here the APS) is responsible for the generation of spatio-temporal patterns in APS. For each simulation, a large number of niches (from 21 to 15 431 472) were created (Table S2). To determine the total number of niches per simulation, we multiplied the number of niches generated for a given dimension by the number generated for all other ecological dimensions. For example, for a run based on temperature, PAR and nitrate (i.e. a 3D run), the total number of niches was 28  $\times$  21  $\times$  27 = 15 876 ecological niches (with 28 niches for SST, 21 for PARc and 27 for nitrate; Table S2). When all

acological dinnersions were considered to \$D25innulation), 27 (nitrate)  $\times$  28 (silicate)  $\times$  27 (phosphate) = 15 431 472 ecological niches (Table S2). Optimum and ecological amplitude of all niches are presented in Table S1.

To test whether niche resolution—function of the increments (Table S2)-affected our analyses, we compared two extreme cases of 1D models (i.e. we named them low and high resolutions hereafter) using each ecological variable. The term "bis" was added to identify high-resolution niches (Tables S2 and S3). Because of the high number of categories generated in the highresolution case (e.g. 144 648 000 categories for simulations based on temperature, PARa and phosphate) and the resulting high computation time, we only performed high-resolution analyses for 1D models.

Finally, annual estimations of pseudo-species abundances were assessed by performing a cubic interpolation of the 1–5D niches with the corresponding environmental variables. Four runs on APS are closely examined as examples: three 1D runs based on either (i) SST, (ii) PAR or (iii) nitrate (Fig. 4) and (iv) one 3D run based on SST, PAR and nitrate (Fig. 5). To reveal the simulated patterns in APS, we also applied a standardized PCA and used the PCs to sort the different pseudo-species in the same way as we did for observed APSs (Step 1). We did one PCA per simulation. In the case of these examples, we therefore performed four PCAs: one for the simulation based exclusively on thermal niches (Fig. 4a-c), one for the simulation based exclusively on PAR niches (Fig. 4d-f), one for the simulation based exclusively on nitrate niches (Fig. 4g-i) and a last one for the simulation based on the 3D (SST, PAR and nitrate) niches (Fig. 5). We only examined significant PCs for which we found correlations >|0.5| between pseudo-species and PCs.

#### Step 4: Comparisons of modelled and observed seasonal patterns

Comparisons between modelled and observed annual patterns in phytoplankton abundance were not based upon regression analyses but assessed by the Pearson's correlation coefficients (Fig. 6 and Fig. 7) and the Mean Absolute Error (MAE; Fig. 7) that measures the average magnitude of the errors in a set of predictions without considering their direction. Equation (3) represents the absolute differences between predictions and observations, divided by the number of differences to be tested (with all individual differences having equal weight)

$$MAE = \sum_{i=1}^{n} \frac{|Xi - Yi|}{n}, \quad (3)$$

with n the number of differences to be tested,  $X_i$  is prediction i and  $Y_i$  is observation i. The MAE is a negatively oriented score; the lower values being related to the strongest correlations.

Pearson's correlation coefficients and MAEs were calculated for each run between all observed and modelled daily patterns in (pseudo-) species abundance, leading to a correlation or MAE matrix [species × pseudo-species]. We then identified the highest positive correlations and the lowest MAE values. For each run and species, and using the average correlation and MAE values, we therefore obtained two vectors (Fig. S4). To graphically depict the relationships, the daily normalized (between 0 and 1) pseudo-species abundances—that showed the highest correlation with observed species—were plotted against daily observed species abundances (Fig. 6).

To consider a possible bias induced by temporal autocorrelation, we tested both correlations and MAEs with null models. First, we randomly generated a number of daily time series corresponding to the total number of pseudo-species generated for each run. The number of time series was small for 1D simulations but became important for an increasing number of dimensions. The procedure was repeated 1000 times and the average Pearson correlation and MAE values were calculated for each simulation. To consider temporal autocorrelation, we generated two million of time series and kept the first 1000 with a 30-order (i.e. 30 days/~1-month autocorrelation for daily time series) autocorrelation higher than average 30-order autocorrelation found in observed daily time series. We represented the results in a diagram that exhibited the observed average correlation for each run and the 1000 correlations found using the null model with (red) and without (blue) autocorrelation (Fig. 7). For each combination of environmental variables (i.e. 84 runs), we calculated the probability of significance of each correlation (Table S3) and used contour diagrams to identify (i) the most important environmental parameters and (ii) the number of dimensions to accurately reconstruct APS. This allowed us to highlight the number of species that exhibits the highest correlations in each run (Fig. 8).

#### **RESULTS**

#### Seasonal changes in environmental parameters in the North Sea

Temperature exhibited a minimum at the beginning of March and a maximum at the end of July-August (Fig. 2). PAR showed minimum and maximum values in December-January and June, respectively. The highest concentrations in nitrate, phosphate and silicate were

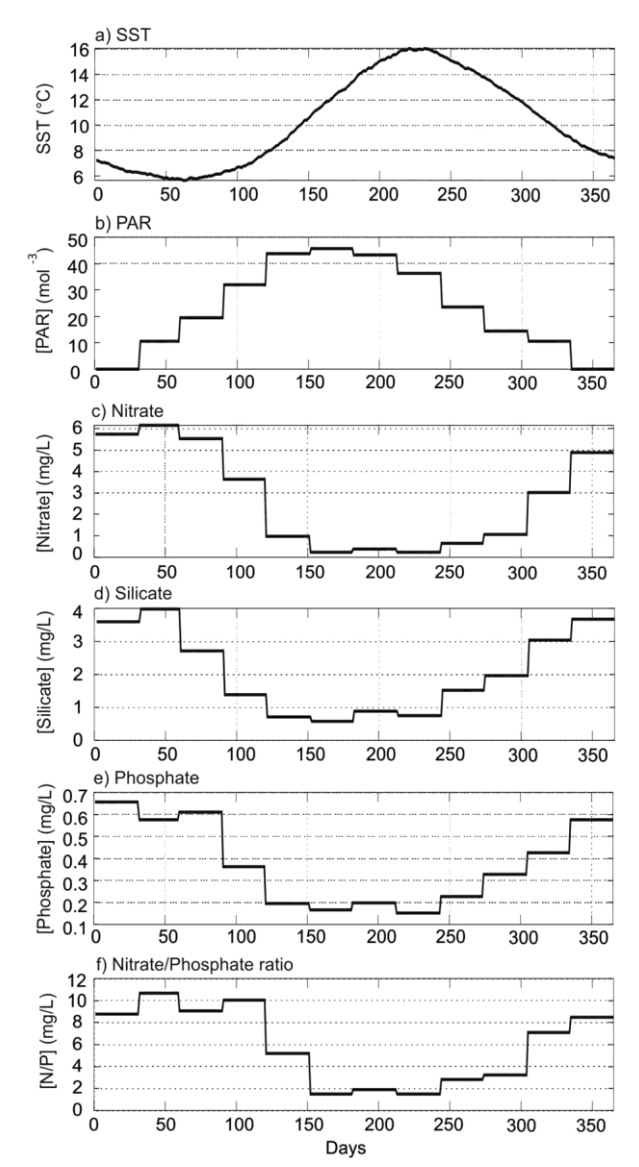


Fig. 2. Annual changes in the environmental parameters considered in this study. (a) SST, (b) PAR, (c) nitrate, (d) silicate, and (e) phosphate concentrations, and (f) nitrate/phosphate (N/P) ratio. Note that SST is at a daily resolution, whereas other parameters are at a monthly one (see Materials and Methods).

observed in winter and reached their lowest concentrations from the end of spring to the end of summer. The MLD reaches the sea floor of the studied area every winter (Fig. S2), shoals in March to reach the shallowest values (i.e. close to 12 m) between April and September.

#### Observed APS

We examined APS based on CPR plankton data by means of a standardized PCA (Fig. 3). The first three PCs were used because they were significant using a broken-stick

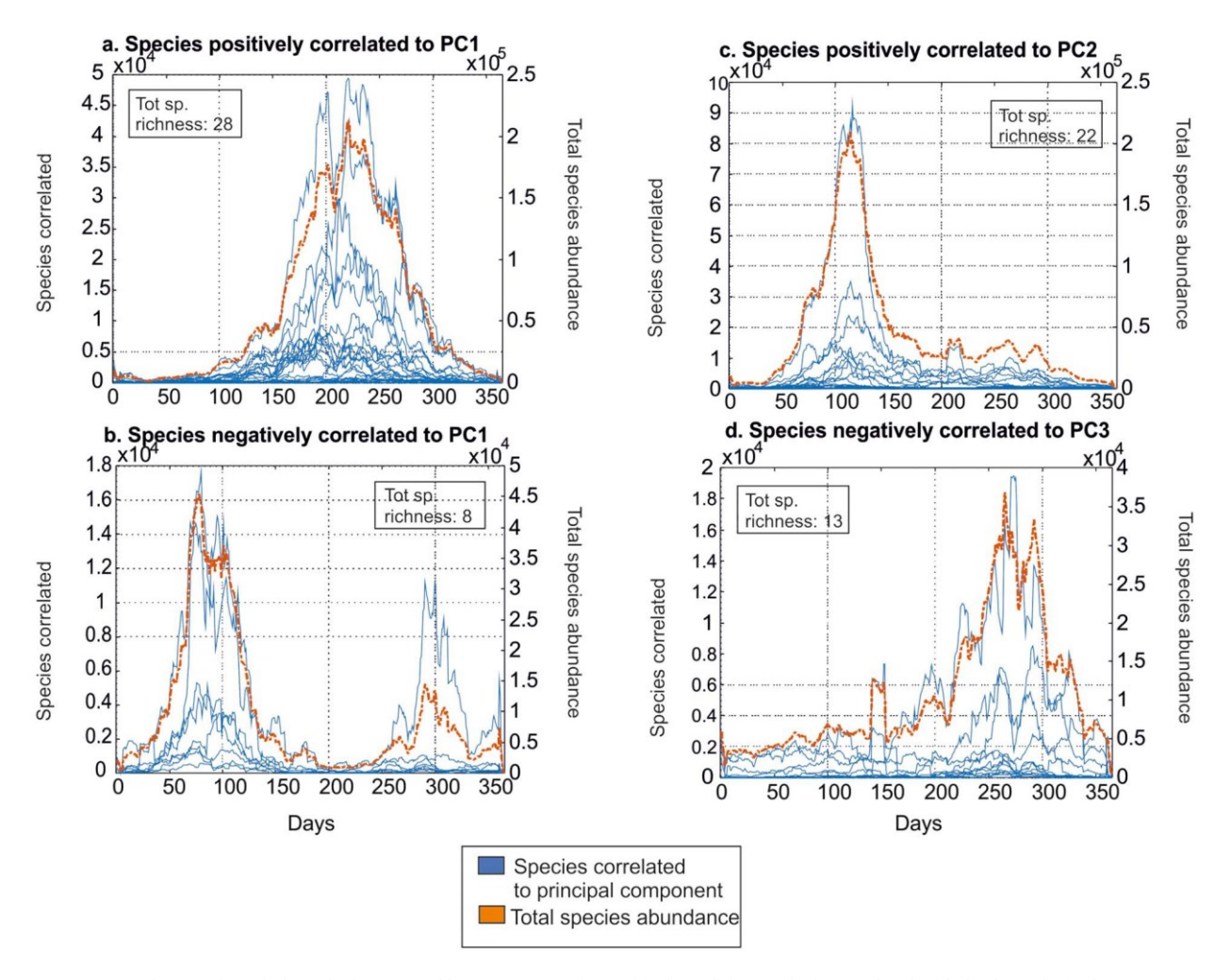


Fig. 3. Annual succession of phytoplankton sorted by PCA. (a) Species positively and (b) negatively correlated with the first principal component (RGH) which are instanced with BCF) of the properties and their relations to the PCs. Tot. Sp. Richness: total species richness.

model with 100 000 simulations (PC1: 26.86%, PC2: 18.06%, PC3: 12.22%; PCs were above the threshold percentage of 6.14, 4.91 and 4.29%, respectively). The PCs allowed us to differentiate five periods, each being characterized by a species assemblage: (i) an early-spring stage (8 species negatively correlated to PC1; left part of Fig. 3b), (ii) a spring stage (22 species positively correlated to PC2; Fig. 3c), (iii) a widespread summer stage (28 species positively related to PC1; Fig. 3a), (iv) a late summer/beginning of autumn stage (13 species negatively correlated to PC3; Fig. 3d) and (v) an autumn stage (8 species negatively correlated to PC1; right part of Fig. 3b). The summer stage (Fig. 3a) was characterized by the highest species richness but showed a low proportion of diatoms in comparison to both spring and autumn stages. Silicoflagellates were also present (Table 1).

#### Modelled APS

We reconstructed APS by using models of growing complexity (i.e. by considering a growing number of niche dimensions) including all combinations of SST, PAR, nitrate, phosphate, silicate and N/P ratio (a total of 84 simulations). Here, we focused on four examples of modelled APS (Fig. 4 and Fig. 5). We used the same procedure (standardized PCA) to sort pseudo-species phenology and characterize annual succession. We retained the first two PCs for simulations based exclusively on thermal niches (81.05 and 15.10% of the explained variance; Fig. 4a–c), for simulations based exclusively on PAR niches (42.98 and 27.66%; Fig. 4d–f) and for simulations based exclusively on nitrate niches (91.84 and 5.10%; Fig. 4g–i). The first four PCs (32.30, 20.90, 14.82 and 11.05%) were kept for simulations based on SST, PAR and nitrate

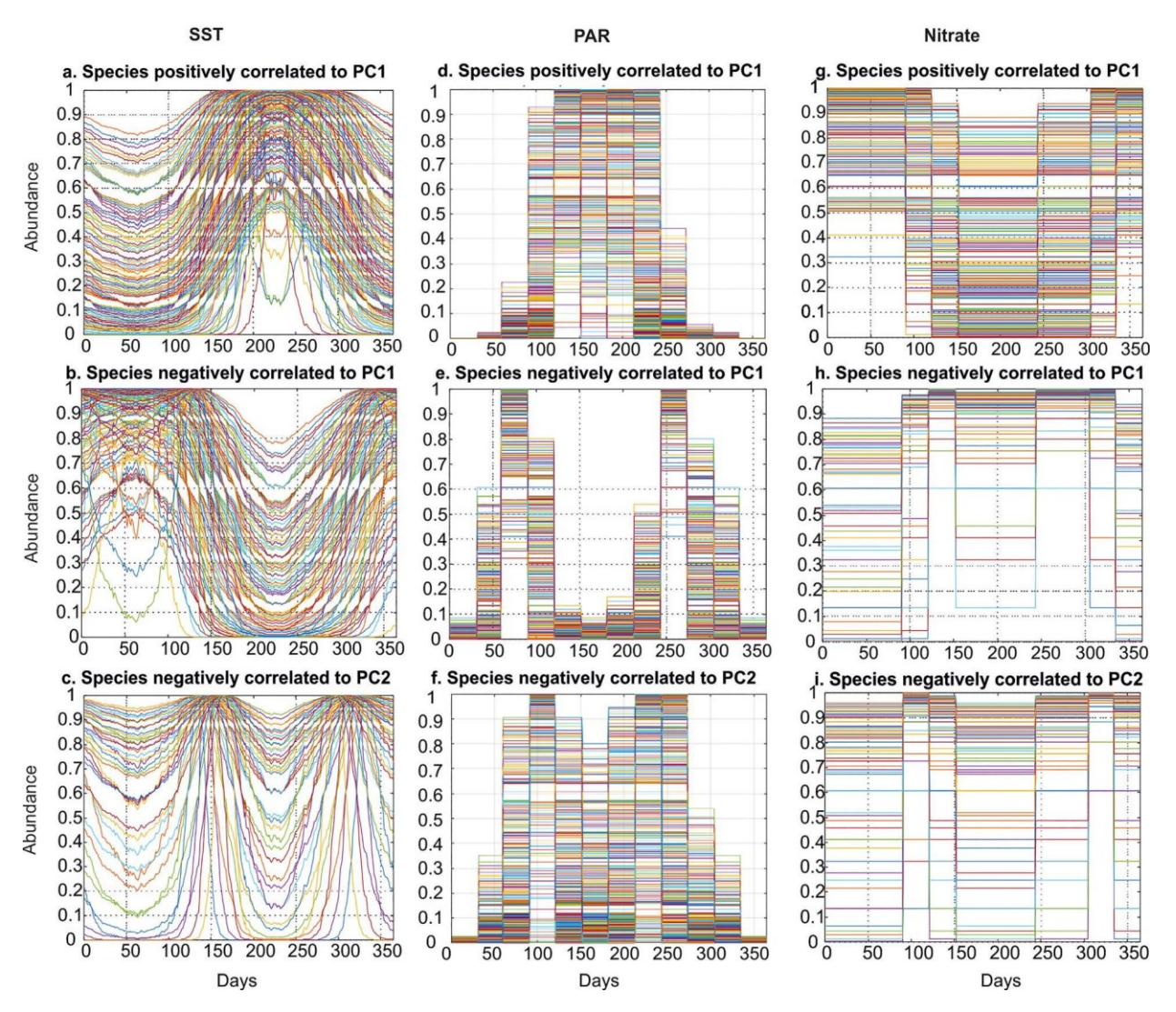


Fig. 4. Reconstructed annual plankton succession from a 1D model based on SST (left panels), PAR (middle panels) and Nitrate (right panels). A PCA was performed on the relative pseudo-species abundances to identify the most important seasonal phytoplankton abundance patterns. Only modelled plankton seasonal changes, related substantially negatively or positively (i.e. normalized eigenvectors > [0.5]) to the PCs, are shown. SST (a-c): species (a) positively and (b) negatively correlated to PC1, and (c) species negatively correlated to PC2. SST: individual pseudo-species abundance is on the left vertical axis. PAR (d-f): species (d) positively and (e) negatively correlated to PC1, and (f) species negatively correlated to PC2. Nitrate (g-i): species (g) positively and (h) negatively correlated to PC1, and (i) species negatively correlated to PC2. Relative individual pseudo-species abundances generated from METAL are on the left vertical axis.

distribution based on 100 000 simulations (thresholds of significance were of 6.14, 4.91, 4.29 and 3.88% for PC1-PC4).

The first simulations, based on thermal niches only, showed two main phases of high phytoplankton abundance (also representative of a high species richness) in summer (Fig. 4a) and winter (Fig. 4b) and two minor phases in spring and autumn (Fig. 4c). The winter phase of high abundance did not correspond to any observed

(Fig. 5), all PCs being significant using the broken-stick patterns (Figs 3 versus 4). The second simulations, based on PAR only, showed several peaks of high phytoplankton abundance in spring, summer and autumn (Fig. 4d-f). These patterns were close to the observed patterns of annual succession (Fig. 3), suggesting an important role of PAR in the modulation of APS. The third simulations based on nitrate only (Fig. 4g-i)—showed an important winter peak in phytoplankton abundance not detected in the observations (Figs 3 versus 4). Considering nitrate only was, therefore, not sufficient to reconstruct APS.

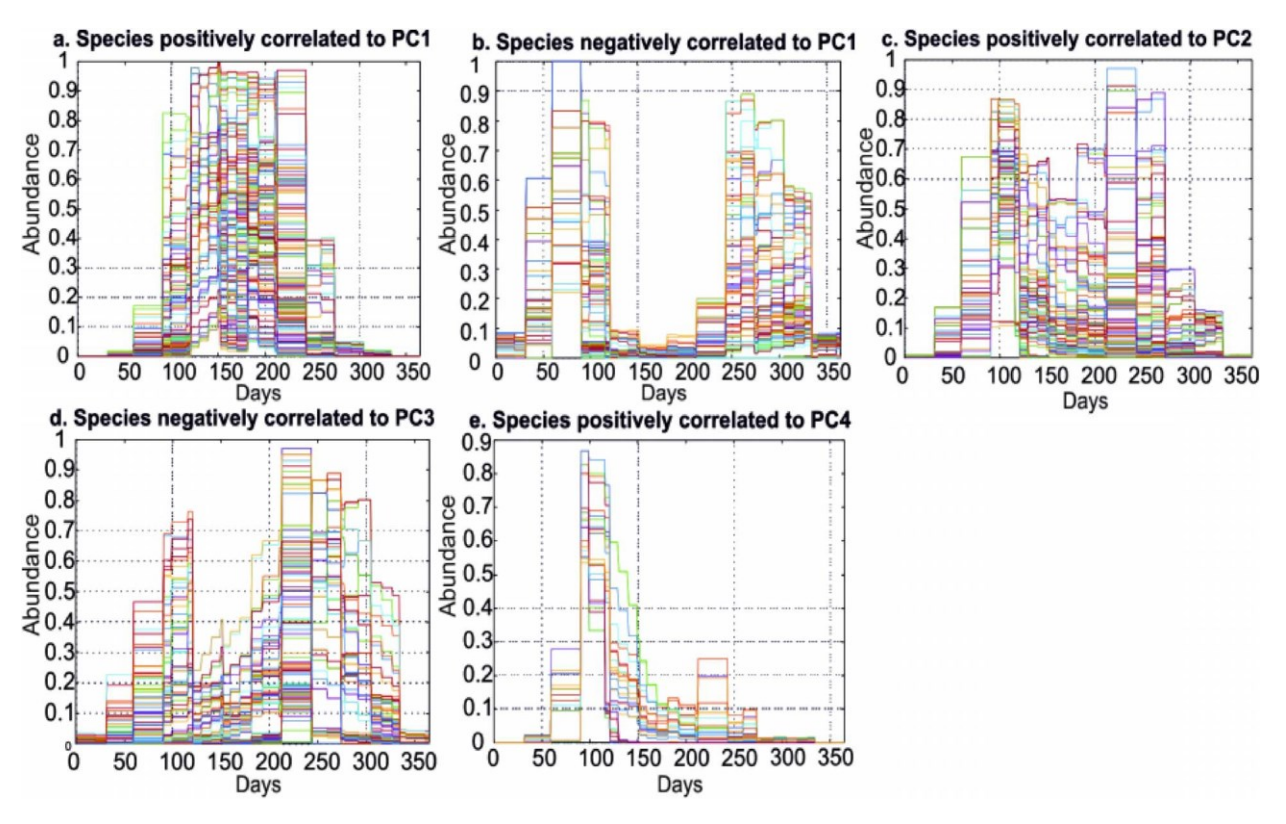


Fig. 5. Reconstructed annual plankton succession from a 3D run based on SST, PAR and Nitrate. A PCA was performed on relative individual pseudo-species abundances to identify the most important seasonal patterns in phytoplankton abundance. Only predicted plankton seasonal changes related substantially negatively or positively (i.e. normalized eigenvectors >|0.5|) to the PCs are shown. Species (a) positively and (b) negatively correlated to PC1. (c) Species negatively correlated to PC3. (e) Species positively correlated to PC4. Individual pseudo-species abundance is on the left vertical axis.

The fourth simulations that combined SST, PAR and nitrate (Fig. 5a-e) were more efficient to reproduce the APS observed in the CPR data, especially during the late-summer phase (Figs 5 versus 3). The relationships between modelled and observed APS are thoroughly examined below.

#### Reconstruction of species seasonal patterns

We calculated the Pearson's correlation coefficients between observed and modelled phytoplankton abundances for the 84 simulations we performed; note that our simulations were characterized by a growing number of ecological dimensions—ranging from one to five—and that all combinations of environmental parameters were tested. We selected the best correlations and examined graphically the relationships (Fig. 6): for most of phytoplankton species or taxa (e.g. Skeletonema costatum and Thalassiosira spp.), pseudo-species reproduced observed seasonal patterns well, while marginal discrepancies were sometimes observed for some species (e.g. Paralia sulcata

and Dactyliosolen antarcticus; Fig. 6). All phytoplankton groups were well modelled (see the colour curves in Fig. 6).

## Identification of the number of ecological dimensions to reconstruct APS

To identify the number of ecological dimensions to use for reconstructing APS well, we calculated—considering all our simulations—the average of the best correlations and MAEs between observed and modelled phytoplankton abundances (Table S3, Fig. 7). We tested the robustness of correlations and MAEs (e.g. possible bias related to temporal autocorrelation) using null models. While MAE values were sometimes significant for 1D simulations (Fig. 7), APS was better reproduced when at least three dimensions were considered (Fig. 7). Not all correlations were significant for models based on three or more ecological dimensions; considering five dimensions did not improve the percentage of explained variance (i.e. model quality). This result emphasizes that using

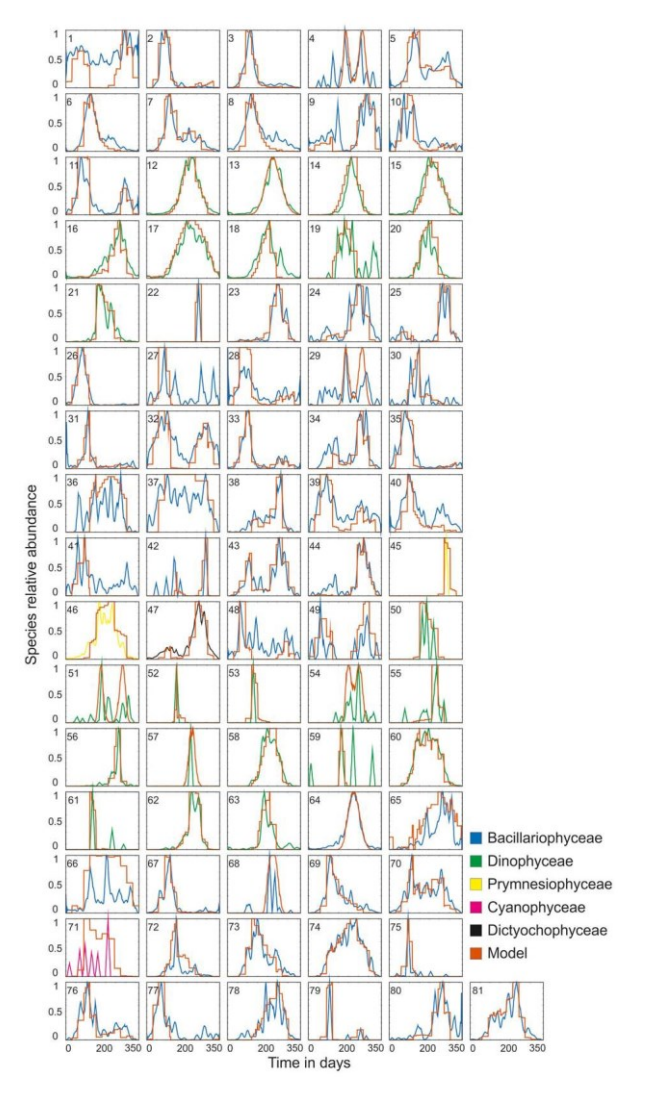


Fig. 6. Seasonal patterns in standardised observed and simulated phytoplankton species abundances. Relative abundances of species sampled by the CPR survey (each taxonomic class being identified by a specific colour, see legend) plotted together with relative abundances of pseudospecies reconstructed using METAL (orange). See Table 1 for species names and taxonomic class.

relevant environmental variables is more important than increasing model complexity.

#### Identification of key environmental variables to reconstruct APS

We then identified the most relevant environmental variables that best reproduce APS and the seasonal patterns that result of species phenology (Fig. 8). Uni-dimensional models (1D, Runs 1–16) explained poorly observed seasonal changes in species abundance, with the exception of Run 2 that was exclusively based on SST (Fig. 8a).

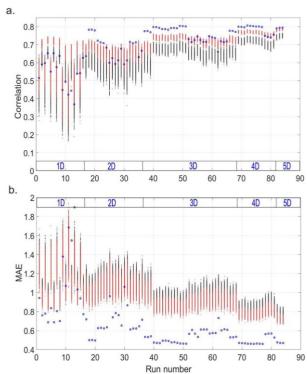


Fig. 7. Average correlation (a) and MAE (b) for each run used to reconstruct APS from 1D to 5D models. The average value (blue circle) was based on the best correlations (a) or MAEs (b) assessed between observed species and (simulated) pseudo-species. Black and red points show the results of the same calculations based on a null model with (red) and without (black) consideration of temporal autocorrelation.

For Run 2, eight species showed their highest correlations between observed and modelled seasonal patterns (Fig. 8a). Two-dimensional models (Runs 17-39) also explained poorly species seasonal patterns and only three species exhibited their highest correlations when simulations were based on both temperature and PAR (Fig. 8a, Table S1). Better results were achieved when models were based on three or more ecological dimensions: 3-5D models showed 29 (Runs 40-68), 25 (Runs 69-81) and 14 (Runs 82-84) highest correlations between observed and modelled seasonal patterns, respectively (Fig. 8a). Note that Run 51, based on SST, N/P and PARc (i.e. a minimum value of PAR =  $20 \text{ E.m}^{-2} \cdot \text{day}^{-1}$ ), exhibited 10 highest correlations.

We also examined the correlations between each simulated and observed seasonal patterns for all species and runs (Fig. 8b). Even if the best results were achieved for models based on SST only (Run 2), results were similar when three or more dimensions were included (Fig. 8b). Low correlations generally appeared when the triplet SST/PAR/macro-nutrient was not used (Fig. 8b and Table S1, e.g. Runs 53-56), revealing that this combination was important to model species seasonal patterns.

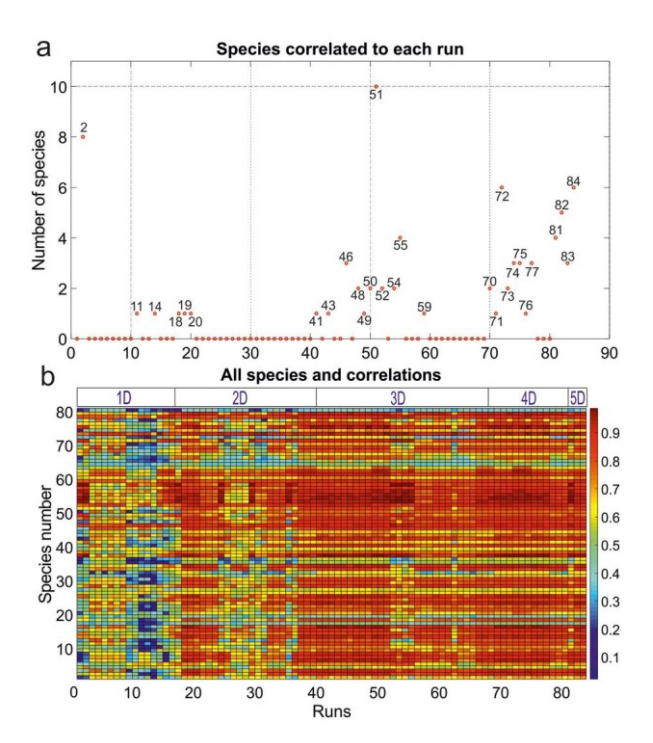


Fig. 8. Identification of the key environmental parameters for reconstructing APS. (a) Number of phytoplankton species exhibiting their highest correlation for each model (run). See Table S1 for the correspondence between run numbers and environmental combinations of variables. (b) Highest correlation for a given phytoplankton species and run. The colorbar shows the linear correlation value.

#### **DISCUSSION**

#### Annual phytoplankton succession

The application of the plankton ecology group (PEG) model in lakes and subsequently in the marine realm (Sommer et al., 1986, 2012) has suggested that (i) physics (light and stratification) controls the start and the end of the phytoplankton growth season, (ii) grazing by metazoan plankton results in a clear water phase, (iii) nutrients define the carrying capacity of phytoplankton, (iv) food limitation determines zooplankton abundance and (v) fish predation determines zooplankton size structure.

While grazing may have a substantial influence on phytoplankton (Kivi et al., 1993; Fileman et al., 2010; Kenitz et al., 2017), its non-consideration in our analyses did not prevent us from accurately reconstructing species phenology. Here, we show that annual plankton succession in the North Sea—including the spring bloom—may originate from the niche-environment interaction with a key role of bottom-up processes in shaping APS, as observed by Romagnan et al. (2015) for the Mediterranean Sea. Our results suggest that PARs, and to a lesser extent SST, are important for the initiation of the spring bloom, macro-nutrients for the end of the spring bloom and both

SST and macro-nutrients for the development of APS. All these parameters (i.e. light, nutrients and temperature) are seen as master parameters controlling photosynthesis in physiological studies (Geider et al., 1997; Longhurst, 1998; McMinn and Martin, 2013; Ras et al., 2013).

In previous works, we suggested that large-scale patterns in biodiversity emerged from the niche-environment interactions that propagate from the species to the community level (Beaugrand, Rombouts, et al., 2013; Beaugrand et al., 2015, 2018, 2020). While APS has been frequently investigated at the group level (e.g. plankton functional type, PEGs or categories), we show that—even within a given ecological or taxonomic group—species reacts to environmental fluctuations individually through the niche-environment interaction, conforming themselves to the principle of species individuality (Whittaker, 1975).

By investigating APS at a species scale, we detected four main microphytoplanktonic successions in the North Sea (see Table 1 for the species list). The first assemblage is composed of species that exhibited their highest abundance at the beginning of spring and a second less important peak in autumn (PC1 in Figs 3b and 6). This microphytoplanktonic assemblage, generally composed of large diatoms such as Thalassionema nitzschioides and Ditylum brightwellii (Table 1 and Fig. 6), was primarily controlled by PAR and nutrients availability. PAR is an essential parameter limiting photosynthesis with a well-known influence on species growth rate (Eppley and Sloan, 1966) that mainly acts in polar regions (McMinn and Martin, 2013), but also in lower latitude areas such as the North Sea (Peeters et al., 1993). The first assemblage is also psychrophilic, reaching its highest (lowest) abundance when temperature is lowest (highest) (Fig. 2). When PAR is highest and when PAR or nutrients concentration is lowest (Fig. 2), the assemblage is not detected, which is consistent with a positive influence of nutrients on both growth rate and primary production (Goldman, 1980; Longhurst, 1998). Although not considered in our simulations (because of data availability), turbulence, mixing and high SST variability, environmental conditions that characterize early spring and autumn may also influence positively the first assemblage which is more adapted to this environment than dinoflagellates (Margalef, 1978; Holligan et al., 1980; Beaugrand et al., 2010). In winter, PAR (or the number of daily light hours) and temperature, to a lesser extent, limit diatom growth; deep-water column mixing combined to an absence of biological production enables nutrients to increase at the surface.

The second assemblage, less psychrophile than the first one and which encompasses species such as *Chaetoceros* spp. or *Coscinodiscus concinnus*, occurs generally between April and June at a time when temperature and PAR

increase, and silicate—and nitrate and phosphate, but to a lesser extent—concentrations diminish (Figs 2, Fig. 3c and Fig. 6).

The third assemblage, mainly composed of dinoflagellates (e.g. Ceratium fusus and Ceratium furca) and of some small diatoms (e.g. Guinardia striata and Guinardia flaccida), is observed in oligotrophic conditions and when temperature and PAR are high (Figs 2, Fig. 3a and Fig. 6). Silicate depletion played an important role in the change in dominance observed between the second and third assemblage. In a mesocosm experiment, silicate deficiency was assumed to be the cause of the strong reduction in large spring bloom diatoms and the replacement by flagellates (Jacobsen et al., 1995). Small diatoms need less silicic acid for their skeleton and have a higher surface to volume ratio which increases nutrient absorption (Miller and Moser, 2004). Dinoflagellates occur in areas when temperatures are warm, SST variability is low and the water column is well stabilized (Margalef, 1978; Beaugrand et al., 2010).

The fourth assemblage is composed of late-summer/ autumn warm-temperate species (e.g. the diatoms Bellerochea malleus and Biddulphia alternans; Figs 3d and 6) with a northern distributional limit in the North Sea (e.g. B. malleus) (Barnard et al., 2004). This assemblage occurs when temperature is high and when nutrients concentration tends to increase.

#### The spring bloom

Our study also provides evidence for a strong environmental control of the initiation, development and termination phases of the spring bloom. The integration of PAR, and to a lesser extent SST, in the simulations can simply explain the initiation of the spring bloom in the North Sea. Average light intensity in the mixed layer is known to govern the timing of the spring bloom (Riley, 1967; Legendre, 1990). This is especially the case in the shallow regions of high latitudes (Reid et al., 1990; Eilertsen, 1993; Shaw and Purdie, 2001). Smyth et al. (2014) have provided evidence that oceanic net heat flux strongly affects ecosystem dynamics and have also conveyed that the spring bloom started in the western part of the English Channel (Station L4, Plymouth) when net heat flux becomes positive (Smyth et al., 2014). Because net heat flux is highly positively correlated with irradiance and PAR (Beaugrand, 2015a), a strong control of PAR on the initiation of the spring bloom may be expected.

The physical structure of the sea water strongly changes at the time of spring bloom initiation, and many studies have suggested that it exerts a strong control,

although the debate remains active on the exact types of physical processes that may play a critical role (Atkinson et al., 2018). Our biological model, however, suggests that APS results from the interaction between niche of species and annual environmental fluctuations. Parameters such as those related to vertical mixing would only affect the abundance by influencing sinking rate and vertical distribution,  $r = \mu - I$  with r the net specific biomass accumulation rate,  $\mu$  the phytoplankton growth rate and I a loss term influenced by sinking and vertical mixing (and other processes such as grazing, respiration and parasitism; Behrenfeld, 2010; Chiswell et al., 2015). In this study, we concentrate on  $\mu$  at the species level and have not implemented any loss rate in our models. We think that this lack of complexity in this shallow region cannot affect our conclusions on the primary control of APS.

Our models suggest that the limitation in macronutrients is a key factor for bloom termination. To model the end of the spring bloom, we did not have to consider the influence of grazing in regulating phytoplankton communities and the exhaustion of surface macronutrients could explain alone bloom termination (Fischer et al., 2014). Large seasonal changes in atmospheric forcing and ocean surface conditions shape, to a large degree, the seasonal cycles of phytoplankton biomass but also the relative abundance of phytoplankton species (Barton et al., 2014). Investigating the oceanic region of the North Atlantic, Beaugrand et al. (2015) showed that phytoplankton and zooplankton seasonal fluctuations were closely related (his figure 5.28), suggesting a bottomup control. More recently, by focusing on a region with approximately the same bathymetry than ours, Atkinson et al. (2018) demonstrated that both the increase and termination of the spring bloom were encapsulated by zooplankton, providing strong evidence against a top-down control.

In the pelagic ecosystem of the North Atlantic, diatom blooms end with the depletion of silicate and are progressively replaced by slower growing dinoflagellates (Taylor et al., 1993). Although the succession between diatoms and dinoflagellates is well explained by macro-nutrients and temperature in our simulations, it is also known since Margalef (1979)—that water column stability is a key factor to explain the succession between these two functional groups. Dinoflagellates are more sensitive than diatoms to turbulence (Karp-Boss et al., 2000). They can undergo significant vertical migrations to nutrient-rich areas but cannot reproduce when turbulence is too high (Estrada and Berdalet, 1997). In contrast, diatoms can continue cell division and the photosynthetic energy products are used to synthesize fatty acid that are converted to energy when cells are exported below the euphotic

zone; fatty acid can be considered as a buoyancy regulator (Amato et al., 2017). It is possible that mixing and turbulence are not required in our models because temperature is a proxy of mixing and turbulence conditions in the North Sea (e.g. Sharples et al., 2006). Confirmation of our results should be searched in regions that experience different sequences of environmental conditions.

#### Uncertainties and potential caveats related to our approach

As with all studies based on modelling and data analysis, it is sometimes difficult to identify primary factors and putative mechanisms at work. In this paper, we have primarily focused on the physical parameters of high biological relevance (temperature, PAR and nutrients; Peeters et al., 1993; Brown et al., 2004; Eilertsen and Degerlund, 2010; Mcminn and Martin, 2013; Behrenfeld and Boss, 2014). We know that these parameters have a key biological role. However, temperature could also be a correlate for another physical parameter of primary importance such as MLD and depth of the euphotic zone (Beaugrand, 2015a). The role of vertical mixing is primarily to increase nutrient concentrations in surface and to influence phytoplankton sinking rate and vertical distribution (Chiswell, 2013; Behrenfeld and Boss, 2014). In the field, natural systems are more complex than models and all parameters act in synergy.

The niche-environment interaction is certainly more unpredictable in the field than in our modelling approach for two main reasons. First, while the fundamental niche (sensy Hutchinson) was estimated here, the environment through random meteorological conditions-may influence the realized niche of microalgae species. Second, phytoplankton community before and/or during the growth of a given species may alter species realized niche by competition for resources that lead to competitive exclusion (Barton et al., 2014). For example, the trait-based approach of Breton et al. (2017) suggests that competitive exclusion prevails during Phaeocystis spp. blooms in the eastern English Channel.

It is well-known that the underwater light available for photosynthesis (PAR) is a key environmental variable for primary production (Cole and Cloern, 1987; MacIntyre et al., 2000; Foden et al., 2010; Capuzzo et al., 2013, 2015, 2018). Light field in the water column depends in turn on phytoplankton biomass (self-shading), inorganic suspended particulate materials, colored dissolved organic materials and water itself (IOCCG, 2000). Recent works on light quality have also revealed the important role of spectral irradiance on phytoplankton succession (Lawrenz and Richardson, 2017). In this study,

we used surface PAR data that originated from a climatology. All phytoplankton species can perform photoregulation or photo-acclimation (i.e. the first occurs at time scales of minutes and the second takes place in a few hours or a day) to limit photo-inhibition in high light surface waters or optimize both light harvesting and Calvin cycle activity in the water column (MacIntyre et al., 2000; Lavaud, 2007; Dubinsky and Stambler, 2009). In addition, photo-acclimation processes can be conducted on different kinetic models and time scales (Cullen and Lewis, 1988), according to environmental conditions and functional phytoplankton groups (MacIntyre et al., 2000). Even if photosynthesis performances between different species remain poorly documented (Goss and Lepetit, 2015; Suggett et al., 2015), they can induce a competitive effect between species at a given time.

#### CONCLUSION

Our study suggests that APS may result from the niche-environment interaction and that APS must be investigated at the species level to accurately explore and understand ecological patterns and processes. Our models provide evidence that sharp temporal environmental gradients may be responsible for the strong annual shifts in microphytoplanktonic composition in the North Sea; this occurs when an environmental factor becomes rapidly favourable (e.g. increasing PAR at the end of winter) or limiting (e.g. diminution of macro-nutrients at the end of spring). We identify the three key parameters that are the best predictors of the succession: (i) temperature, (ii) PAR and (iii) macro-nutrients. There is a clear effect of temperature on APS with a cline from coldwater species in early spring to warm-water species in late summer. By enabling the initiation of the spring bloom and ending the second bloom in autumn, PAR exerts a pivotal role. Macro-nutrients are critical at the end of the spring bloom and their increases in autumn trigger a secondary bloom which then becomes rapidly limited by conditions in PAR and temperature. Mixing is an important process by which macro-nutrients increase in the euphotic zone.

#### ACKNOWLEDGEMENTS

The CPR Survey is an internationally funded charity that operates the CPR programme. The CPR survey operations and routes are funded by a funding consortium from the UK, USA, Canada and Norway. Within the UK, government organizations DEFRA and NERC contribute to core operations. Part of this research was funded by the Centre National de la Recherche Scientifique (CNRS). This research was funded as part of the ANR TROPHIK and the programme CLIMIBIO.

#### REFERENCES

- Amato, A., Dell'Aquila, G., Musacchia, F., Annunziata, R., Ugarte, A., Maillet, N., Carbone, A., Ribera d'Alcalà, M. et al. (2017) Marine diatoms change their gene expression profile when exposed to microscale turbulence under nutrient replete conditions. Sci. Rep., **3826**, 1–11.
- Asrar, G., Myneni, R. B., Li, Y. and Kanemasu, E. T. (1989) Measuring and modeling spectral characteristics of a tallgrass prairie. Remote Sens. Environ., 27, 143-155.
- Atkinson, A., Polimene, L., Fileman, E. S., Widdicombe, C. L., McEvoy, A. J., Smyth, T. J., Djeghri, N., Sailley, S. F. et al. (2018) What drives plankton seasonality in a stratifying shelf sea? Some competing and complementary theories. Limnol. Oceanogr., 63, 2877-2884.
- Barnard, R., Batten, S. D., Beaugrand, G., Buckland, C., Conway, D. V. P., Edwards, M., Finlayson, J., Gregory, L. W. et al. (2004) Continuous plankton records: plankton atlas of the North Atlantic Ocean (1958-1999). II. Biogeographical charts. Mar. Ecol. Prog. Ser., MEPS supplement, 11–75.
- Barton, A. D., Lozier, M. S. and Williams, R. G. (2014) Physical controls of variability in North Atlantic phytoplankton communities. Limnol. Oceanogr., 60, 181-197.
- Beaugrand, G., Ibañez, F. and Reid, P. C. (2000) Long-term and seasonal fluctuations of plankton in relation to hydroclimatic features in the English Channel, Celtic Sea and Bay of Biscay. Mar. Ecol. Prog. Ser., **200**. 93–102.
- Beaugrand, G., Reid, P. C., Ibañez, F., Lindley, J. A. and Edwards, M. (2002) Reorganization of North Atlantic marine copepod biodiversity and climate. Science, 296, 1692-1694.
- Beaugrand, G., Luczak, C. and Edwards, M. (2009) Rapid biogeographical plankton shifts in the North Atlantic Ocean. Glob. Chang. Biol., 15,
- Beaugrand, G., Edwards, M. and Legendre, L. (2010) Marine biodiversity, ecosystem functioning and the carbon cycles. Proc. Natl. Acad. Sci. USA, 107, 10120-10124.
- Beaugrand, G., Mackas, D. and Goberville, E. (2013) Applying the concept of the ecological niche and a macroecological approach to understand how climate influences zooplankton: advantages, assumptions, limitations and requirements. Prog. Oceanogr., 111, 75-90.
- Beaugrand, G., Rombouts, I. and Kirby, R. R. (2013) Towards an understanding of the pattern of biodiversity in the oceans. Glob. Ecol. Biogeogr., 22, 440-449.
- Beaugrand, G., Goberville, E., Luczak, C. and Kirby, R. R. (2014) Marine biological shifts and climate. Proc. Royal Soc. B, 281, 20133350.
- Beaugrand, G., Edwards, M., Raybaud, V., Goberville, E. and Kirby, R. R. (2015) Future vulnerability of marine biodiversity compared with contemporary and past changes. Nat. Clim. Chang., 5, 695-670.
- Beaugrand, G. (2015a) Marine Biodiversity. Climatic Variability and Global Change, Routledge, London.
- Beaugrand, G. (2015b) Theoretical basis for predicting climate-induced abrupt shifts in the oceans. Philos. T. R. Soc. B, 370, 20130264.
- Beaugrand, G. and Kirby, R. R. (2018) How do marine pelagic species respond to climate change? Theories and observations. Ann. Rev. Mar. Sci., 10, 169-197.
- Beaugrand, G., Luczak, C., Goberville, E. and Kirby, R. R. (2018) Marine biodiversity and the chessboard of life. PLoS One, 13, e0194006.
- Beaugrand, G., Conversi, A., Atkinson, A., Cloern, J., Chiba, S., Fonda-Umani, S., Kirby, R. R., Greene, C. H. et al. (2019) Prediction of

- unprecedented biological shifts in the global ocean. Nat. Clim. Chang., 9, 237-243.
- Beaugrand, G., Kirby, R. R. and Goberville, E. (2020) The mathematical influence on global patterns of biodiversity. Ecol. Evol., 10,
- Behrenfeld, M. J. (2010) Abandoning Sverdrup's critical depth hypothesis on phytoplankton blooms. Ecology, 91, 977–989.
- Behrenfeld, M. J. and Boss, E. S. (2014) Resurrecting the ecological underpinnings of ocean plankton blooms. Ann. Rev. Mar. Sci., 6, 167-194.
- Breton, E., Christaki, U., Bonato, S., Didry, M. and Artigas, L. F. (2017) Functional trait variation and nitrogen use efficiency in temperate coastal phytoplankton. Mar. Ecol. Prog. Ser., 563, 35-49.
- Brown, J. H., Gillooly, J. F., Allen, A. P., Savage, V. M. and West, G. B. (2004) Toward a metabolic theory of ecology. Ecology, 85, 1771–1789.
- Capuzzo, E., Painting, S. J., Forster, R. M., Greenwood, N., Stephens, D. T. and Mikkelsen, O. A. (2013) Variability in the sub-surface light climate at ecohydrodynamically distinct sites in the North Sea. Biogeochemistry, 113, 85-103.
- Capuzzo, E., Stephens, D., Silva, T., Barry, J. and Forster, R. M. (2015) Decrease in water clarity of the southern and central North Sea during the 20th century. Glob. Chang. Biol., 21, 2206-2214.
- Capuzzo, E., Lynam, C., Barry, J., Stephens, D., Forster, R. M., Greenwood, N., McQuatters-Gollop, A., Silva, T. et al. (2018) A decline in primary production in the North Sea over 25 years, associated with reductions in zooplankton abundance and fish stock recruitment. Glob. Chang. Biol., 24, 352-364.
- Chiswell, S. M. (2011) Annual cycles and spring blooms in phytoplankton: don't abandon Sverdrup completely. Mar. Ecol. Prog. Ser., 443, 39-50.
- Chiswell, S. M. (2013) Comment on "annual cycles of ecological disturbance and recovery underlying the subarctic Atlantic spring plankton bloom". Global Biogeochem. Cy., 27, 1291–1293.
- Chiswell, S. M., Calil, P. H. R. and Boyd, P. W. (2015) Spring blooms and annual cycles of phytoplankton: a unified perspective. J. Plankton Res., 37, 500-508.
- Cole, B. E. and Cloern, J. E. (1987) An empirical model for estimating phytoplankton productivity in estuaries. Mar. Ecol. Prog. Ser., 36, 299-305.
- Colebrook, J. M. (1979) Continuous plankton records: seasonal cycles of phytoplankton and copepods in the North Atlantic Ocean and the North Sea. Mar. Biol., 51, 23-32.
- Colebrook, J. M. (1982) Continuous plankton records: seasonal variations in the distribution and abundance of plankton in the North Atlantic Ocean and the North Sea. J. Plankton Res., 4, 435-462
- Colebrook, J. M. (1984) Continuous plankton records: relationships between species of phytoplankton and zooplankton in the seasonal cycle. Mar. Biol., 83, 313-323.
- Cullen, J. J. and Lewis, M. R. (1988) The kinetics of algal photoadaptation in the context of vertical mixing. J. Plankton Res., 10, 1039-1063.
- Cushing, D. H. (1959) The seasonal variation in oceanic production as a problem in population dynamics. ICES J. Mar. Sci., 24, 455-464.
- Dakos, V., Beninca, E., VAN Nes, E. H., Philippart, C. J. M., Scheffer, M. and Huisman, J. (2009) Interannual variability in species composition explained as seasonally entrained chaos. Proc. Royal Soc. B, 276, 2871-2880.

- Dubinsky, Z. and Stambler, N. (2009) Photoacclimation processes in phytoplankton: mechanisms, consequences, and applications. Aquat. Microb. Ecol., 56, 163-176.
- Eilertsen, H. C. (1993) Spring blooms and stratification. Nature, 363, 24.
- Eilertsen, H. C. and Degerlund, M. (2010) Phytoplankton and light during the northern high-latitude winter. J. Plankton Res., 32, 899-912.
- Eppley, R. W. and Sloan, P. R. (1966) Growth rates of marine phytoplankton: correlation with light absorption by cell chlorophyll A. Physiol. Plant., 19, 47-59.
- Estrada, M. and Berdalet, E. (1997) Phytoplankton in a turbulent world. Sci. Mar., 61, 125-140.
- Falkowski, P., Scholes, R. J., Boyle, E., Canadell, J., Canfield, D., Elser, J., Gruber, N., Hibbard, K. et al. (2000) The global carbon cycle: a test of our knowledge of earth as a system. Science, 290, 291-296.
- Falkowski, P. G. and Oliver, M. J. (2007) Mix and match: how climate selects phytoplankton. Nat. Rev. Microbiol., 5, 813-819.
- Fileman, E., Petropavlovsky, A. and Harris, R. (2010) Grazing by the copepods Calanus helgolandicus and Acartia clausi on the protozooplankton community at station L4 in the western English Channel. J. Plankton Res., 32, 709-724.
- Fischer, A. D., Moberg, E. A., Alexander, H., Brownlee, E. F., Hunter-Cevera, K. R., Pitz, K. J., Rosengard, S. Z. and Sosik, H. M. (2014) Sixty years of Sverdrup: a retrospective of progress in the study of phytoplankton blooms. Oceanography, 27, 222-235.
- Foden, J., Devlin, M. J., Mills, D. K. and Malcolm, S. J. (2010) Searching for undesirable disturbance: an application of the OSPAR eutrophication assessment method to marine waters of England and Wales. Biogeochemistry, 106, 157–175.
- Frontier, S. (1976) Etude de la décroissance des valeurs propres dans Une analyse en composantes principales: comparaison avec le modèle du bâton brisé. J. Exp. Mar. Biol. Ecol., 25, 67-75.
- Garcia, H. E., Locarnini, R. A., Boyer, T. P., Antonov, J. I., Baranova, O. K., Zweng, M. M., Reagan, J. R. and Johnson, D. R. (2014) World Ocean Atlas 2013: volume 4: dissolved inorganic nutrients (phosphate, nitrate, silicate). In S. Levitus (Eds.), 4, 25.
- Gauch, H. G., Chase, G. B. and Whittaker, R. H. (1974) Ordination of vegetation samples by Gaussian species distributions. Ecology, 55, 1382-1390.
- Geider, R. J., MacIntyre, H. L. and Kana, T. M. (1997) A dynamic model of phytoplankton growth and acclimation: responses of the balanced growth rate and chlorophyll a: carbon ratio to light, nutrient-limitation and temperature. Mar. Ecol. Prog. Ser., 148, 187-200.
- Gilbert, J. A., Steele, J. A., Caporaso, J. G., Steinbrück, L., Reeder, J., Temperton, B. and Somerfield, P. J. (2012) Defining seasonal marine microbial community dynamics. ISME J., 6, 298–308.
- Goldman, J. C. (1980) Physiological processes, nutrient availability, and the concept of relative growth rate in marine phytoplankton ecology. In Falkowski, P. G. (ed.), Primary Productivity in the Sea, Plenum, New York, pp. 179-194.
- Goss, R. and Lepetit, B. (2015) Biodiversity of NPQ. J. Plant Physiol., **172**. 13–32.
- Helaouët, P. and Beaugrand, G. (2009) Physiology, ecological niches and species distribution. Ecosystems, 12, 1235-1245.
- Holligan, P. M., Maddock, L. and Dodge, J. D. (1980) The distribution of dinoflagellates around the British Isles in July 1977: a multivariate analysis. J. Mar. Biol. Assoc. UK, 60, 851-867.

- Hubbell, S. P. (2001) The Unified Neutral Theory of Biodiversity and Biogeography, Princeton University Press, Princeton.
- Huisman, J., VAN Oostveen, P. and Weissing, F. J. (1999) Critical depth and critical turbulence: two different mechanisms for the development of phytoplankton blooms. Limnol. Oceanogr., 44, 1781-1787.
- Hutchinson, G. E. (1957) Concluding remarks. Cold Spring Harb. Symp. Quant. Bio., 22, 415-427.
- Huthnance, J. M. (1991) Physical oceanography of the North Sea. Ocean. Shore. Manag., 16, 199–231.
- IOCCG (2000) Remote sensing of ocean colour in coastal, and optically-complex, waters. In Reports of the International Ocean-Colour Coordinating Group, Vol. 3, Sathyendranath, S, IOCCG, Dartmouth, Canada.
- Jacobsen, A., Egge, J. K. and Heimdal, B. R. (1995) Effects of increased concentration of nitrate and phosphate during a spring bloom experiment in microcosm. J. Exp. Mar. Biol. Ecol., 187, 239-251.
- Jolliffe, I. T. (1986) Principal Component Analysis. Springer series in statistics. Springer, New York, NY.
- Karp-Boss, L., Boss, E. and Jumars, P. A. (2000) Motion of dinoflagellates in simple shear flow. Limnol. Oceanogr., 45, 1594-1602.
- Kenitz, K., Visser, A., Mariani, P. and Andersen, K. H. (2017) Seasonal succession in zooplankton feeding traits reveals trophic trait coupling. Limnol. Oceanogr., 62, 1184-1197.
- Kivi, K., Kaitala, S., Kuosa, H., Kuparinen, J., Leskinen, E., Lignell, R., Marcussen, B. and Tamrninen, T. (1993) Nutrient limitation and grazing control of the Baltic planktonic community during annual succession. Limnol. Oceanogr., 38, 893–905.
- Lavaud, J. (2007) Fast regulation of photosynthesis in diatoms: mechanisms, evolution and ecophysiology. Funct. Plant Sci. Biotechnol., 1, 267-287.
- Lawrenz, E. and Richardson, T. L. (2017) Differential effects of changes in spectral irradiance on photoacclimation, primary productivity and growth in Rhodomonas salina (cryptophyceae) and Skeletonema costatum (bacillariophyceae) in simulated black water environment. J. Phycol., **53**, 1241-1254.
- Legendre, L. (1990) The significance of microalgal blooms for fisheries and for the export of particulate organic carbon in oceans. J. Plankton Res., 12, 681-699.
- Legendre, P. and Legendre, L. (1998) Numerical Ecology, 2nd English edn, Elsevier Amsterdam.
- Levin, S. A. and Lubchenco, J. (2008) Resilience, robustness, and marine ecosystem-based management. Bioscience, 58, 27-32.
- Longhurst, A. (1998) Ecological Geography of the Sea, Elsevier. Academic Press, London.
- MacIntyre, H. L., Kana, T. M. and Geider, R. J. (2000) The effect of water motion on short-term rates of photosynthesis by marine phytoplankton. Trends Plant Sci., 5, 12-17.
- Mann, K. H. and Lazier, J. R. N. (1996) Dynamics of Marine Ecosystems: Biological-Physical Interactions in the Oceans, 2nd edn, Blackwell Science,
- Margalef, R. (1978) Life-forms of phytoplankton as survival alternatives in an unstable environment. Oceanol. Acta, 1, 493-509.
- Margalef, R. (1979) Functional morphology of organisms involved in red tides, as adapted to decaying turbulence. Toxic dinoflagellate blooms, 1, 89-94.
- McMinn, A. and Martin, A. (2013) Dark survival in a warming world. Proc. Royal Soc. B., 280, 20122909.

- Metaxas, A. and Scheibling, R. E. (1996) Top-down and bottom-up regulation of phytoplankton assemblages in tidepools. Mar. Ecol. Prog. Ser. 145, 161–177.
- Miller, J. H. and Moser, S. (2004) Communication and coordination. Complexity, 9, 31-40.
- Peeters, J. C. H., Haas, H. A., Peperzak, L. and De Vries, I. (1993) Nutrients and light as factors controlling phytoplankton biomass on the Dutch continental shelf (North Sea). In 1988-1990. Report DGW-93.004, Rijkswaterstaat tidal waters division, Middelburg.
- Pingree, R. D., Holligan, P. M. and Mardell, G. T. (1978) The effects of vertical stability on phytoplankton distributions in summer on the northwest European shelf. Deep-Sea Res., 25, 1011-1028.
- Ras, M., Steyer, J. P. and Bernard, O. (2013) Temperature effect on microalgae: a crucial factor for outdoor production. Rev. Environ. Sci. Biotechnol., 12, 153-164.
- Redfield, A. (1958) The biological control of chemical factors in the environment. Am. Sci., 46, 205-221.
- Reid, P. C., Lancelot, W. W. C., Gieskes, E., Hagmeier, E. and Weickart, G. (1990) Phytoplankton of the North Sea and its dynamics: a review. Neth. J. Sea Res., 26, 295-331.
- Reid, P. C., Edwards, M., Hunt, H. G. and Warner, A. J. (1998) Phytoplankton change in the North Atlantic. Nature, 391, 546.
- Reid, P. C., Colebrook, J. M., Matthews, J. B. L., Aiken, J., Barnard, R., Batten, S. D., Beaugrand, G., Buckland, C. et al. (2003) The continuous plankton recorder: concepts and history, from plankton indicator to undulating recorders. Prog. Oceanogr., 58, 117-173.
- Reynolds, R. W., Rayner, N. A., Smith, T. M., Stokes, D. C. and Wang, W. (2002) An improved in situ and satellite SST analysis for climate. J. Climate, 15, 1609-1625.
- Riley, G. A. (1967) The plankton of estuaries. In: Lauff, G. H. (ed). Estuaries. Washington, DC. Amer. Assoc. Adv. Sci., 83, 316-326.
- Romagnan, J. B., Legendre, L., Guidi, L., Jamet, J. L., Jamet, D., Mousseau, L., Pedrotti, M. L., Picheral, M. et al. (2015) Comprehensive model of annual plankton succession based on the wholeplankton time series approach. PLoS One, 10, e0119219.
- Sharples, J., Ross, O. N., Scott, B. E., Greenstreet, S. P. R. and Fraser, H. (2006) Inter-annual variability in the timing of stratification and the spring bloom in the northwestern North Sea. Continent Shelf Res, **26**, 733–751.

- Shaw, P. J. and Purdie, D. A. (2001) Phytoplankton photosynthesisirradiance parameters in the near-shore UK coastal waters of the North Sea: temporal variation and environmental control. Mar. Ecol. Prog. Ser., 216, 83-94.
- Smyth, T. J., Allen, I., Atkinson, A., Bruun, J. T., Harmer, R. A., Pingree, R. D., Widdicombe, C. E. and Somerfield, P. J. (2014) Ocean net heat flux influences seasonal to interannual patterns of plankton abundance. PLoS One, 9, e98709.
- Sommer, U., Gliwicz, Z., Lampert, W. and Duncan, A. (1986) The pegmodel of seasonal succession of planktonic events in fresh waters. Arch. Hydrobiol., 106, 433-471.
- Sommer, U., Adrian, R., De Senerpont Domis, L., Elser, J. J., Gaedke, U., Ibelings, B., Jeppesen, E., Lürling, M. et al. (2012) Beyond the plankton ecology group (PEG) model: mechanisms driving plankton succession. Annu. Rev. Ecol. Evol. Syst., 43, 429-448.
- Suggett, D. J., Goyen, S., Evenhuis, C., Szabo, M., Pettay, D. T., Warner, M. E. and Ralph, P. J. (2015) Functional diversity of photobiological traits within the genus Symbiodinium appears to be governed by the interaction of cell size with cladal designation. New Phytol., 208, 370-381.
- Sverdrup, H. U. (1953) On conditions for the vernal blooming of phytoplankton. J. Cons. Int. Explor. Mer., 18, 287-295.
- Ter Braak, C. J. F. (1996) Unimodal models to relate species to environment, Agricultural Mathematics Group, Wageningen, The Netherlands.
- Thackeray, S. J., Henrys, P. A., Hemming, D., Bell, J. R., Botham, M. S., Burthe, S., Helaouët, P., Johns, D. G. et al. (2016) Phenological sensitivity to climate across taxa and trophic levels. Nature, 535, 241-245.
- Widdicombe, C. E., Eloire, D., Harbour, D., Harris, R. P. and Somerfield, P. J. (2010) Long-term phytoplankton community dynamics in the western English Channel. J. Plankton Res., 32, 643-655.
- Whittaker, R. H. (1975) Communities and Ecosystems, 2nd edn, Macmillan, New York.
- Winder, M. and Cloern, J. E. (2010) The annual cycles of phytoplankton biomass. Philos. T. R. Soc. B, 365, 3215-3226.
- Zhai, L., Platt, T., Tang, C., Sathyendranath, S. and Walne, A. (2013) The response of phytoplankton to climate variability associated with the North Atlantic oscillation. Deep-Sea Res. Pt. II, 93, 159-168.